(A New Proposal to Jefferson Lab PAC27)

High resolution study of the resonance in nK^+ system

J. P. Chen, E. Chudakov, C. DeJager, P. Degtyarenko, R. Feuerbach, M. Jones, J. Gomez, O. Hansen, D. W. Higinbotham, J. LeRose, R. Michaels, S. Nanda, B. Reitz, A. Saha, B. Wojtsekhowski (contact and spokesperson)
Thomas Jefferson National Accelerator Facility, Newport News, VA 23606

J. Arrington, K. Hafidi, R. Holt, P. E. Reimer(co-spokesperson), D. Potterveld, E. Schulte, X. Zheng
Argonne National Laboratory, Argonne, IL 60439

G. Cates(co-spokesperson), D. Day, A. Deur, R. Lindgren, N. Liyanage, V. Nelyubin(co-spokesperson)†, B. E. Norum, J. Singh, R. Snyder, W. A. Tobias, K. Wang
University of Virginia, Charlottesville, VA 22901

D. Nikolenko, I. Rachek, Yu. Shestakov
Budker Institute, Novosibirsk, Russia

. D. J. Magaziotis .
California State University LA, CA

G. B. Franklin, B. Quinn
Carnegie Mellon University, Pittsburgh, PA 15213

L. Pentchev
College of William and Mary, Williamsburg, VA 23185

P. Markowitz, J. Reinhold
Florida International University, Miami, FL 33199

E. Cisbani, F. Cusanno, F. Garibaldi, S. Frullani, G. M. Urciuoli, M. Iodice
INFN, Rome, Italy

R. De Leo, L. La Gamba
INFN, Bari, Italy

A. Asratyan, G. Davidenko, A. Dolgolenko, G. Dzyubenko, V. Evdokimov, V. Goryachev, M. Kubantsev, I. Larin, V. Matveev, A. Sitnikov, V. Verebryusov, V. Vishnyakov
Institute of Experimental and Theoretical Physics, Moscow, Russia

W. Bertozzi, O. Gayou, S. Gilad, Y. Qiang
Massachusetts Institute of Technology, Cambridge, MA 02139

K. Hicks
Ohio University, Athens, OH 45701

Ya. Azimov
PNPI of Russian Academy of Science, Gatchina, Russia

V. Koubarovski, P. Stoler
Rensselaer Polytechnic Institute, Troy, NY 12180-3590

R. Gilman
Rutgers, The State University of New Jersey, Piscataway, NJ 08854

P. Souder, R. Holmes, H. Benaoum .
Syracuse University, Suracuse, NY 13244

E. Piasetzky
Tel Aviv University, Israel

W. Briscoe, R. Arndt, I. Strakovsky, R. Workman
Center for Nuclear Studies, Department of Physics
The George Washington University, Washington DC 20052

S. Dhamija, W. Korsch
The University of Kentucky, Lexington, KY 40506

J. Annand, D. Ireland, J. Kellie, K. Livingston, G. Rosner
University of Glasgow, Glasgow, Scotland

A.M. Nathan
University of Illinois, Champaign-Urbana, IL 61801

K. Kumar, K. Paschke, L. Kaufman
University of Massachusets, Amherst, MA

J. Calarco, W. Hersman
University of New Hampshire, Durham, NH 03824

K. Egiyan, S. Mayilyan, V. Mamyan, A. Shahinyan, H. Voskanyan
Yerevan Physics Institute, Yerevan, Armenia

and **The Hall A Collaboration**
† on leave from PNPI of Russian Academy of Sciences, Gatchina, Russia
* also TJNAF, Newport News, VA 23606

December 6, 2004

Abstract

An experiment is proposed to search for and measure the parameters of a narrow exotic baryonic state in reaction Be$(e, nK^+K^-)X$ in the mass range from 1500 to 1600 MeV. The data will determine the resonance mass and width with a detector resolution (FWHM) of 2.1 MeV. The width will be determined with accuracy of 0.7 MeV for 3 MeV wide resonance.

The experiment utilizes a 5.0 GeV electron beam in Hall A, High Resolution Spectrometer (left) with a septa magnet, the BigBite spectrometer, and a large neutron detector. This equipment exists or is under construction for the approved experiment E02013. With 550 hours of beam-time for this measurement, resonances whose widths as small as 1 MeV may be observed unambiguously. Such a measurement will dramatically increase our experimental confidence in the parameters of the exotic state Θ^+ and its nature.

Contents

1 Introduction

After two years, the existence of the Θ^+ pentaquark state remains highly controversial[1]. Whereas many experiments have seen evidence supporting the existence of the Θ^+[3, 4, 5, 6, 7, 8, 9, 10], none has had sufficient statistical significance to make the observation overwhelmingly convincing. In fact, as experimental information accumulates, there are even some potential inconsistencies in the data. Still, however, the quality, and the shear quantity, of the various experiments has left the question of the Θ^+'s existence very much alive. Interest in the community has been fueled by the profound implications for QCD should the pentaquark be confirmed beyond doubt.

Evidence for the Θ^+ was first reported by SPring-8[3]. Its width was determined to be something under 25 MeV, a measurement that was limited by experimental resolution. The observation was consistent with a particle with $S = +1$ and a quark content of $uudd\bar{s}$. Such a state was predicted as a member of an antidecuplet of the flavor group $SU(3)_F$ [2]. The predicted width was around 15 MeV, consistent with the observation. Soon thereafter the DIANA Collaboration reported seeing a similar state in bubble chamber data on K^+Xe scattering[4]. Again the measurement of the width was limited by experimental resolution, which this time was around 9 MeV. The CLAS Collaboration at JLab also saw the state in exclusive photoproduction from the deuteron with a quoted width of 21 MeV, again limited by experimental resolution. Toward the end of 2003, it is probably fair to say that there was a bias toward the notion that if the Θ^+ is real it must have a width of around 10-20 MeV.

Today, the experimental picture is very different from that of a year ago. It can be argued that if the Θ^+ is real, it must have a width that is at most a few MeV. With such a narrow width, there are fairly stringent theoretical constraints on the size of the cross section. At the same time, SPring-8 simply could not have seen a signal if the cross section were too small. This establishes a window in cross section, which if eliminated, would cleanly kill the existence of the Θ^+. Conversely, if the Θ^+ is real, measurements that are sensitive to that range will provide a clean and unambiguous confirmation.

Our experiment will use a berylium target to study the reaction $e\,n \rightarrow e\,K^-\,\Theta^+ \rightarrow e\,K^-\,K^+\,n$, something that is quite close to the reaction $\gamma\,n \rightarrow K^-\,\Theta^+ \rightarrow K^-\,K^+\,n$ that was studied at SPring-8 except that the photon in our case is virtual. The experiment takes advantage of the large acceptance of the neutron detector that is being built for E02-013, and the bigbite spectrometer that is being built for several experiments. The fortuitous availability of these substantial pieces of equipment, together with the Hall A septum magnet and one of the HRS's, results in an experiment with excellent statistical precision as well as the best instrumental resolution of any pentaquark study to date, 2.3 MeV.

Before continuing, we emphasize one final point. There is no current approved experiment, including those being conducted at CLAS, that is capable of killing the Θ^+. Without our experiment, it is likely that the question of the possible existence of the Θ^+ will remain unaswered for years, something that would be bad for the progress of our field.

1.1 The width of the Θ^+ and the implications for cross section

In the later part of 2003 and during 2004, evidence accumulated that put more stringent limits on the width of the Θ^+. For instance, Arndt, Strakovsky and Workman published a phase-shift analysis of old K^+p and K^+d data in which they exclude any features such as the Θ^+ with widths above a few MeV[17]. Another constraint follows from the fact that for

K^+d resonant elastic scattering, the integrated cross section is entirely determined by the resonance's width and spin. Nussinov took advantage of this by using data from the Particle Data Handbook on total cross section for K^+d scattering to determine that the width of the Θ^+ $\Gamma < 6\,\mathrm{MeV}$[16]. Cahn and Trilling made a similar analysis of the aforementioned K^+Xe collisions[18]. While there are some uncertainties regarding rescattering in the Xe nucleus, they concluded that $\Gamma = 0.9 \pm 0.3\,\mathrm{MeV}$.

While the constraints on the width of the Θ^+ from elastic K^+d scattering has a theoretical transparency that Jaffe has referred to as "gold plated"[19], there are other measurements that provide information that is at least "silver plated"[19]. The COSY-TOF collaboration reported a narrow resonance consistent with the Θ^+ in the reaction $p\,p \to \Sigma^+\,K^0\,p$[10]. While their experimental resolution was only about 18 MeV, they also reported a cross section of $0.4 \pm 0.1(\mathrm{stat}) \pm 0.1(\mathrm{syst})\,\mu\mathrm{b}$. Liu and Ko have calculated the cross section for the COSY reaction using a hadronic Lagrangian with couplings that are empirically constrained by various experiments[20]. In comparing the COSY data with Liu and Ko's calculation, one is led to the conclusion that $\Gamma \sim 8\,\mathrm{MeV}$.

These experiments, taken at face value, give a range of roughly $1\,\mathrm{MeV} < \Gamma < 8\,\mathrm{MeV}$. It is also possible that one experiment or another that saw a positive signal was a statistical fluctuation which would push the limits on the width or cross section to smaller values. We are thus left with two important questions. Is the original SPring-8 observation consistent with such a small cross section? And if so, what kind of experiment could definitively settle the issue of whether or not the Θ^+ exists? Unfortunately, the SPring-8 collaboration did not publish even an order-of-magnitude estimate of their observed cross section. Even so, we can conservatively estimate a range of possibilites from their published data.

1.2 Is SPring-8 consistent with subsequent observations/analyses?

In analyzing their data, the SPring-8 collaboration identified two collections of events in which, among other criteria, a K^+ and a K^- were identified in the final state[3]. The two groups of events differed in that in one group, a proton was seen in a silicon-strip vertex detector, and in the other group, the proton hit was missing. The first group was believed to be rich in events corresponding to the reaction

$$\gamma\,p \to K^+\,\Lambda(1520) \to K^+\,K^-\,p \quad .$$

Indeed, when the missing mass $MM^c_{\gamma\,K^+}$ was contructed, a peak was seen at 1520 MeV. When the same missing mass was constructed for the group without the proton hit, no such peak was seen. They argued that the proton veto was effective in suppressing events corresponding to the production of a Λ. They also looked at the missing mass $MM^c_{\gamma\,K^-}$. For the events without the proton in the final state, a peak was seen at 1540 MeV. They interpreted these events as being due to the reaction:

$$\gamma\,n \to K^-\,\Theta^+ \to K^+\,K^-\,n$$

To increase their confidence that these events were due to the formation of a Θ^+, they looked at a corresponding group of events from an upstream liquid hydrogen target. No such peak was seen in those events.

It is reasonable to argue that the acceptance for these two reactions is quite similar. In both cases a K^+ and a K^- are detected in the final state, and the efficiency of the proton veto must be fairly good or it would not suppress the events containing a Λ. The total cross section for the production of Λ's at SPring-8's photon energies is on the order of 1000 nb, and they detected around 30 events. Since they detected around 36 Θ^+'s, it is not unreasonable to assume that the cross section implied for the Θ^+ would naively be about the same.

Next, one might ask whether the cross section for producing the Θ^+'s could be smaller. For instance, one could imagine that for some reason the Θ^+'s are produced in a very forward direction. At one extreme, you might imagine that *all* of the Θ^+'s are detected, but only a fraction of the Λ's. The SPring-8 detector subtends about 3% of the full solid angle. One could conservatively assume that at least 3% of the Λ's are detected. This would imply a total cross section for Θ^+'s of 30 nb. This is awfully conservative. Surely if we argued that the total cross section σ_0 for the process observed by SPring-8 falls in the range $10\,\text{nb} < \sigma_0 < 1000\,\text{nb}$, where the extremes are very unlikely, we would be safe. Thus, an experiment with good sensitivity at the level of 10 nb would either provide a definitive observation, or a limit on cross section that effectively kills the SPring-8 result.

We return now to the question of whether the SPring-8 result is consistent with subsequent experiments and reanalyses of old data. Liu and Ko have calculated the cross sections for photoproduction of Θ^+'s off neutrons[21]. For a width of 20 MeV, they compute a peak cross section around 300 nb. Accordingly, a cross section of 10 nb would imply a width of around 0.67 MeV. A calculation by Guidal, Polyakov, and Vanderhaeghen has a peak cross section of around 160 MeV for a width of 20 MeV[45]. In this case a cross section of 10 nb would imply a width of about 1.25 MeV. Thus, taking the full range of cross sections discussed above ($10\,\text{nb} < \sigma_0 < 1000\,\text{nb}$) and the range found by the two calculations, we find that the cross section observed at SPring-8 implies that $0.7\,\text{MeV} < \Gamma < 125\,\text{MeV}$ where either extreme is extremely unlikely, but something inbetween might be permitted. Apparently, just barely, the process observed by SPring-8 might be consistent with the limits that are imposed by kaon scattering data.

1.3 A quick snapshot of the proposed experiment

The proposed experiment will be performed using one of the JLab Hall A spectrometers (to detect the K^-), the new BigBite spectrometer (to detect the K^+) and the new large neutron detector that is being built for E02-013[24]. The Hall A spectrometer will be used in conjunction with one of the new septum magnets, allowing the K^- to be detected at 6°. The value of the Θ^+ mass will also be accurately measured with the use of several methods for calibration of the detector system. Our instrumental width will be around 2.1 MeV, allowing us to determine the width to about 0.5 MeV.

If the process observed by SPring-8 had a cross section of 10 nb, where the central photon energy was just over 2 GeV, our cross section should be anywere from 2-5 nb with a central photon energy of around 4 GeV. The range given depends on whether we consider the calculation of Liu and Ko or that due to Guidal, Polyakov and Vanderhaeghen. Even with 2 nb, we would still see an effect of over 11 σ. The absence of an effect would preclude cross sections above about .5 nb at something like a 99% confidence level, solidly showing that the effect in SPring-8 was either an artifact or a fluctuation. No other experiment can say this, including CLAS. Under appropriate circumstances CLAS is capable of confirming the Θ^+, but there are many ways in which a negative result from CLAS would leave open the question of the Θ^+'s existence.

Approach/ Collaboration	Beam/Target	Channel	Mass (MeV)	Width (MeV)	Events in Signal/Background	Ref.
Theoretical Predictions						
Chiral soluton			1530	<15		[2]
Experimental Observations						
LEPS	$\gamma^{12}C$	nK^+	1540±10	<25	19/17	[3]
DIANA	K^+Xe	pK_s°	1539±2	<9	29/44	[4]
CLAS/γn	γD	nK^+	1542±5	<21	43/54	[5]
CLAS/γp	γH	nK^+	1555±16	<26	41/28	[6]
ELSA	γH	nK^+	1540±4±2	<25	55/56	[7]
ITEP/ν	$\nu H, D, Ne/H$	pK_s°	1533±5	<20	26/15	[8]
HERMES	eD	pK_s°	1526±2±2	<24	74/145	[9]
COSY	pp	$K^\circ p\Sigma^-$	?	<18	62/112	[10]
SVD	pA	$K^\circ pX$	?	<15	50/78	[11]
Limits based on *Non*-Observations						
USC	K^+d		1543	<6	—	[16]
GWU	K^+n		1540−1550	≤1	—	[17]
Jülich	K^+n		1545	<5	—	[22]
Approved experiments and some proposals						
Approach/ Collaboration	Beam/Target	Channel	Mass (MeV)	Expected resolution	Events in Signal/Background	Ref.
LEPS D run	γD	nK^+K^-	—	10-15	100 2/1	[25]
CLAS, g10	γD	nK^+	—	10-20	1000 2/1	[26]
CLAS, g11	γH	nK^+	—	10-20	1000 2/1	[27]
M2-HallA	eD	epK^-	—	2.8	520(50nb) 4/1	[28]
M1-HallA	eBe	nK^+K^-	—	2.9	300(4.5nb) 2/1	this proposal

Table 1: Theoretical predictions, experimental observations and limits based on non-observation for the production of the Θ^+.

1.4 The impact of this experiment

In summary, experimental evidence, taken at face value, suggests that the width of the Θ^+ must be in the range $1\,\mathrm{MeV} < \Gamma < 8\,\mathrm{MeV}$. If some of the observations turned out to be anamalous, the width could be even smaller. The effect seen at SPring-8, on the other hand, almost certainly has a total cross section larger than 10 nb. Depending on theoretical assumptions, the width could be as small as 0.67 MeV. Taking into account the dependence on photon energy, a cross section at SPring-8 of 10 nb would translate into 2-5 nb of cross section in our experiment. Even a 2 nb effect would be visible at the 11 σ level. PR04-112 can provide definitive evidence that will either support or refute the SPring-8 result.

1.5 The organization of this proposal

The proposal is organized as follows. In section 1 we present the physics motivation and the goals of the proposed experiment. Section 2 introduces the kinematics of the proposed measurements. In section 3 we describe essential features of both the standard and the specialized equipment. Section 4 deals with calculations and recent experimental data on single rates on the detectors. Section 5 presents a Monte Carlo simulation study. Section 6 presents the details of proposed measurements, the resulting mass resolution, event rates and analysis. Section 7 presents the detailed plan of the equipment calibration based of several independent schemes. Expected results and a beam time request are shown in section 9. Finally the proposal is summarized in section 10.

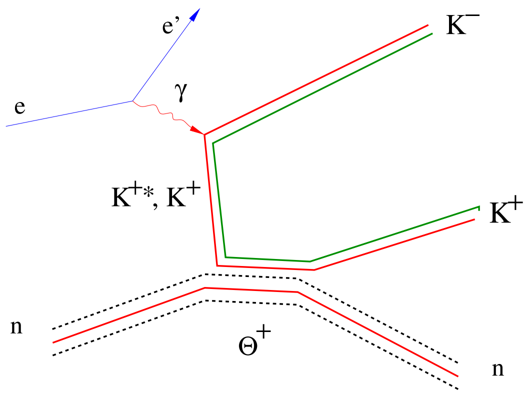

Figure 1: The diagram of the Θ^+ production process.

2 Kinematics

The diagram of the reaction is shown in Fig. 1. The quasi-real photons are produced by electron scattering. A pair of kaons is produced through the diffractive mechanism with t-channel dominance. The virtual kaon interaction with a neutron results in the Θ^+. The Θ^+ state decays into a neutron and a K^+. The narrow width of the Θ^+ means that its decay is most likely to happen at a large distance from the target nuclei. The reaction is characterized by forward angle between negative kaon and photon momenta. The dominant exchange particles are the pseudo-scalar K^+ and, less important, the much more massive vector K^{+*}.

As illustrated in Figs. 2 this experiment will study production of the Θ^+ from a Be target. The high-energy negative kaon (or electron) will be detected in the Left High Resolution Spectrometer (HRS-left) at a central angle of 6° with a septum magnet. The electron (a negative kaon in the parasitic electro production measurement) will remain undetected. Both decay products of the Θ^+ will be detected and provide full information about the Θ^+ four-momentum. The positive kaon will be detected in the BigBite spectrometer at horizontal/vertical angles 18.4°/-20°, and the neutron will be detected in the large neutron detector at horizontal/vertical angles 18.4°/+20° (see Fig. 2). Distance from the target center to the BigBite iron is of 2.3 m, which is larger that standard distance of 1.07 m. Distance from the target center to the neutron detector is of 12 m as it will be in GEN experiment.

An electron beam with a current of 30 μA at an energy of 5.0 GeV will be used. The Be target of total thickness 1.5 mm will be made of 20 foils with spacing of 25 mm. Such configuration allows effective rejection of the accidental events from different targets and minimization of the multiple scattering in the target.

HRS-left is selected for kaon detection because it is equipped with threshold Čerenkov counters for pion rejection at the trigger level and the state-of-the art RICH detector for identifying the kaon [31]. High momentum kaon leads to a slowdown of the Θ^+ particle and better resolution for its mass. The direction of the Θ^+ particle is about 18°. The relatively small momentum of the produced Θ^+ (of 1 GeV/c) and low energy yield in its decay to the nK^+ channel leads to a large angle between K^+ and neutron. The forward direction of the Θ^+ leads to positioning the detectors in a place with high background rate, especially if

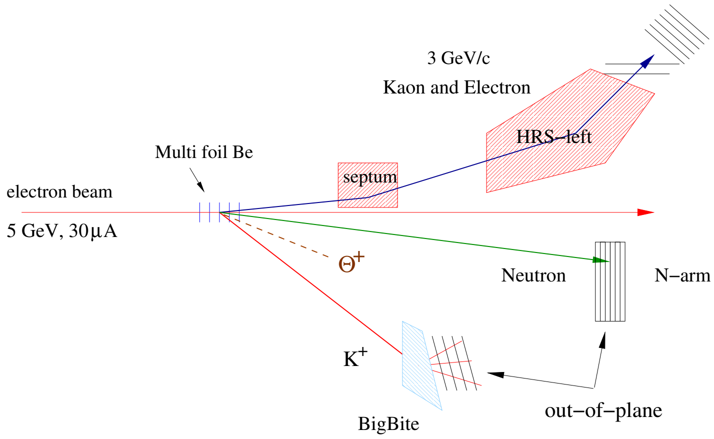

Figure 2: The experimental setup in this experiment.

the detectors are located in the same plane as the negative kaon. So, we plan to put both detectors for decay products out-of-plane. The BigBite will be installed in the Θ^+ direction down by 20° and the neutron detector in the Θ^+ direction up by 20°. Such an arrangement has a relatively large angle between the beam line and detectors (20-35°) and also a large range of angles between the Θ^+ momentum and decay products (due to the favorable aspect ratio of the acceptance in BigBite and the neutron detector) which is very important for determining the resonance spin. The choice of 5.0 GeV electron beam energy (0.5 GeV higher than in the proposal [28]) allows for the parallel study of the electro production of the Θ^+ state.

item	value
central momentum range, p_c [GeV/c]	0.3-4.3
momentum acceptance, $\Delta p/p_c$ [%]	$\pm$ 4.5
momentum resolution, σ_p/p	$1.1 \cdot 10^{-4}$
minimum angle for the central trajectory	6° with septum
solid angle for the point target [msr]	6.2 (4.3 with septum)
coverage for scattering angle	3.1°
extended target acceptance, Y [cm]	$\pm$ 5
θ_{disp} angular resolution (rms) [mr]	1.5
$\theta_{nondisp}$ angular resolution (rms) [mr]	2.0
target vertex Y resolution, σ_Y [mm]	1.5
path from the target to the trigger [m]	25 (27 with septum)
detector area (front chamber), [cm x cm]	200×15
trigger segmentation	16
time resolution, σ_{ToF} [ns]	0.15

Table 2: The parameters of the HRS spectrometer.

3 Experimental Setup

The experiment will be performed in Hall A, where most of equipment needed in this proposed experiment already exists or will be ready soon for experiment E02-013, scheduled to start installation in the fall of 2005.

3.1 The CEBAF electron beam

The beam energy of 5.0 GeV with relatively low beam current of 30 μA will be used in this experiment.

3.2 The target

The experiment will utilize a standard Hall A solid target ladder with Be target and a 4 cm long liquid hydrogen cell (with current of 30 μA) for calibration measurements. The Be target will consists of twenty 75 μm foils spaced by 25 mm. Made of 5 mm wide vertical strips such a target provides a thickness of 275 mg/cm^2. Because of large length it allows effective rejection of the accidental coincidence events between HRS and BigBite by using a target vertex test and at the same time the small thickness in the way of particles allows low momentum kaons to be detected without significant multiple scattering.

3.3 The High Resolution Spectrometer-left

Basic parameters of the HRS-left are given in Tab. 2. The spectrometer has very good momentum and angular resolutions and moderate momentum and angular acceptances.

In this experiment for PID in the HRS-left, we are going to use a combination of the RICH, the gas threshold Čerenkov counter, two layer shower detector, and time-of-flight (ToF) on 27 meter path from the target to the S2m scintillator plane. The gas Čerenkov counter filled with either C_4F_{10} or freon-114 will have very good pion rejection at momentum above 2.8 GeV/c. Electrons will be identified by a large signal in the shower detector or in the gas Čerenkov counter with efficiency of 99.9%. The expected few percent pion contamination

item		value
nominal momentum coverage (at H=9 kG)	[GeV/c]	0.4-1.0
momentum resolution, σ_p/p	[%]	0.4
solid angle for the 50 cm long target	[msr]	26
θ angular resolution	[mr]	0.15
vertical angular resolution	[mr]	0.20
target vertex resolution, σ_z	[mm]	5
path from the target to the trigger	[m]	4.7
detector area (front chamber),	[cm x cm]	140×35
detector area (back chamber),	[cm x cm]	200×50

Table 3: The parameters of the BigBite spectrometer from MC simulation of this experiment (230 cm from the target to the magnet).

in the electron event sample will be reduced by the shower counter by a factor 30-50. Kaons will be identified by absence of the signal in the gas Čerenkov counter, a small signal in the shower detector and correct value of the Čerenkov angle in the RICH detector [31]. Difference in ToF between the pions and the kaons at 3.0 GeV/c momentum is about 1.1 ns, which provides an additional pion (and electron) rejection factor of 5 for ToF resolution (sigma) of 0.30 ns, which has already been achieved.

3.4 The BigBite spectrometer

The BigBite spectrometer consists of a 20 ton dipole magnet and its detector system, which includes planes of drift chambers and trigger/PID counters. The concept of such a spectrometer was developed and realized at NIKHEF [32]. The parameters obtained for the detection of kaons (MC simulation) in present experiment are given in Tab. 3. For operation in Hall A at higher luminosity, the original detector system is being modified. The new detector has a set of high resolution drift chambers. The particle path from the target to the front wire chamber of BigBite will be in vacuum. MC studies have been done for the geometry of the present proposal for the detection of the K^+. For 600 MeV/c momentum kaon, the relative momentum resolution was found to be 0.4% and an angular resolution of 0.2 mr.

BigBite is equipped with a two-layer scintillator trigger plane, which provide 0.20 ns ToF resolution and $\Delta E/E$ information. Two layers segmented Čerenkov counters with a water radiator (similar to that built for HKS [33]) and the aerogel radiator (n = 1.055, similar to the A2 detector in HRS-left) will be added to the BigBite detector package. Table 4 shows the calculated number of photo-electrons in the Čerenkov counters and the ToF difference between kaon and pion for different momenta. The water Čerenkov detector will be used for off-line positive identification of kaons at momenta above 600 MeV/c. Protons with momenta below 600 MeV/c will be rejected using ToF. Particle identification in the proposed counters in BigBite was also studied by using GEANT-3 MC code.

3.5 The neutron detector

The large neutron detector is under construction for experiment E02013 [24]. The detector test assembly will be done in spring 2005. It consists of 244 neutron bars and 184 veto paddles. They are arranged in seven(six) layers with the iron converters and two veto planes.

momentum	average number of photo electrons					Δ ToF
[MeV/c]	p in water	K in water	K in aerogel	π in water	π in aerogel	$K-\pi$ [ns]
200	0	0	0	150	0	23.8
400	0	0	0	340	0	15.9
600	0	50	0	370	15	8.5
800	0	200	0	380	22	5.2
1000		270	0	390	24	3.5

Table 4: The light collection (the average number of photo-electrons) in the Čerenkov counters and the difference between ToF for K and π in BigBite.

Figure 3 shows the schematic view of the detector cross section. The detector efficiency for the neutron with the trigger threshold of 20 MeVee, averaged over energy range of present proposal, is 25.3%, which takes into account a significant loss of neutrons from interactions in the front shielding and interactions which fire the corresponding veto counters. Each neutron bar is viewed by two PMTs, so the ToF resolution (rms) is better then 0.30 ns. Because the neutron energy in the proposed experiment is much less than in GEN the trigger threshold will be reduced from 50 MeV to 20 MeV. We also plan to reduce thickness of the steel plates (neutron converters), which also hold the plastic bars, from 1 inch to 0.5 inch. The detector efficiency as calculated with a GEANT-4 based code is shown in Fig. 4 for different threshold levels.

A trigger scheme of the neutron arm is based on summing the signals from all counters of four vertical layers (total 32 bars) as shown in Fig. 3. The PMT signals in each two layers are summed together (denoted as SS1-15) and then used for the overlapping sums (denoted as S1-14). The output signals from S1-14 units will be discriminated and form the neutron arm trigger.

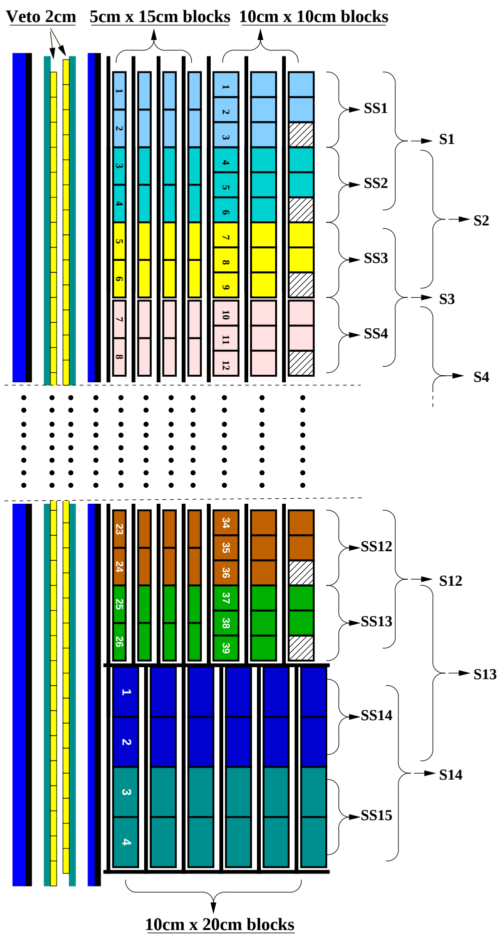

Figure 3: The scheme of the neutron detector and the groups of the counters whose signals will be summed for use in the trigger.

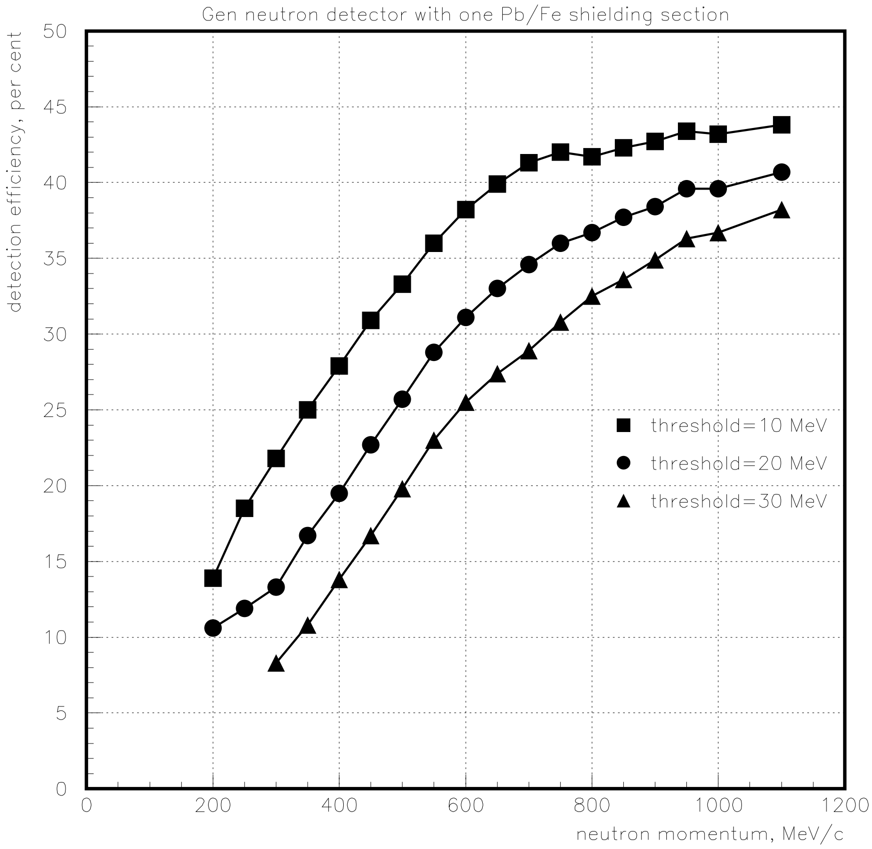

Figure 4: The efficiency of the neutron detector for different threshold levels.

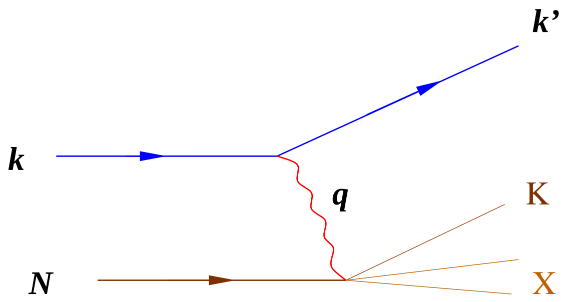

Figure 5: Kinematics quantities for description of electron-nucleon scattering: k and k' are the four-momenta of incoming and outgoing electrons, N is the four-momentum of a nucleon with mass M. The exchange photon transfers four-momentum $q = k - k'$ to the target.

4 Inclusive electro-production

In this section the inclusive reactions, which define the singles rates of electrons, pions, kaons and protons in the spectrometers, are presented. In both the BigBite and the neutron arm detectors the rates dominate in the low energy part of the particle spectra. We used a DINREG-based code [34] for the calculation of the low energy part of the inclusive spectra ($E_{hadron} << E_{beam}$). DINREG reproduced published neutron and proton yields in electro-nuclear reactions [35]. DINREG-based calculations for the wire chamber rates were found to be in agreement with measurements in Hall A [37].

The HRS-left will be used to detect negatively charge particles with a momentum of about 3.0 GeV/c. Electron yield was found from a DIS parametrization and checked relatively to direct measurement in Hall A. The yields of negative pions and kaons were calculated by using the parametrization from Wiser's thesis [39] and checked relatively results from DESY and SLAC measurements of inclusive photo-production [40, 41, 42].

4.1 Kinematics and definitions

The kinematic quantities of electro-production are presented in Fig. 5.

The definitions of the kinematical variables are given for the reaction $e + N \rightarrow e' + K + X$. The five four-momenta involved are:

$$\begin{aligned} k &= (E, \vec{k}), \text{ for the incident electron} \\ k' &= (E', \vec{k'}), \text{ for the scattered electron} \\ N &= (M, \vec{P}), \text{ for the target nucleon} \\ K &= (E_K, \vec{p}_K), \text{ for the produced kaon} \\ X &= (E_X, \vec{p}_X), \text{ for the residual system} \end{aligned}$$

A few kinematic variables are defined below as:

$$\begin{aligned} q^2 &= (k - k')^2 = -Q^2, \\ \nu &= E - E', \\ \epsilon &= \left[1 + 2\frac{\nu^2+Q^2}{Q^2} tan^2\frac{\theta_e}{2}\right]^{-1}, \\ W^2 &= (q + N)^2, \end{aligned}$$

$$t \;=\; (q\;-\;K)^2,$$

$$x_{_F} \;=\; p^{cm}_{_{K,z}}/p^{cm}_{_{K,z\,max}}, \text{ the Feynman variable}$$

The differential cross section of inelastic eN scattering processes is written in the usual notation as

$$\frac{d^2\sigma}{dE'd\Omega_{e'}} \;=\; \frac{\alpha^2}{4E^2sin^4(\frac{\theta}{2})}\left[W_2(q^2,\nu)cos^2(\tfrac{\theta}{2}) + 2W_1(q^2,\nu)sin^2(\tfrac{\theta}{2})\right].$$

In the approximation of $E, E' >> M_N$ and finite q^2, ν we will use

$$\frac{d^2\sigma}{dE'd\Omega_{e'}} \;\approx\; \frac{\alpha^2}{4E^2sin^4(\frac{\theta}{2})}\frac{F_2(q^2,\nu)}{\nu}.$$

The differential cross section for the electro-production of the kaon can be presented as:

$$\frac{d^3\sigma}{dE'd\Omega_{e'}d\Omega_{_K}} = \Gamma\cdot\frac{d\sigma_{\gamma^*,K}}{d\Omega_{_K}},$$

where Γ is the virtual photon flux factor, given by:

$$\Gamma \;=\; \frac{\alpha}{2\pi^2}\frac{E'}{E}\frac{W^2-M^2}{2MQ^2}\frac{1}{1-\epsilon},$$

and $\frac{d\sigma_{\gamma^*,K}}{d\Omega_{_K}}$ is the cross section for kaon production by the virtual photon. At small scattering angle, where $Q^2 << \nu^2$, the transverse terms of the cross section are dominate, so we will use the form:

$$\frac{d\sigma_{\gamma^*,K}}{d\Omega_{_K}} \;=\; \frac{d\sigma_{_T}}{d\Omega_{_K}} \;+\; \epsilon\;\frac{d\sigma_{_{TT}}}{d\Omega_{_K}}\;cos(2\phi),$$

where ϕ is the angle between the electron scattering plane and the Θ^+ production plane.

4.2 Singles rates in the HRS

In the present experiment the HRS will be at 6° and the central momentum at 3.0 GeV/c. The kinematics for the beam energy of 5 GeV corresponds to Q^2 of 0.15 (GeV/c)^2. An electron rate is of 120 kHz for the luminosity of $\mathcal{L}_{eN}$ of $3\cdot 10^{37}$ cm^{2}s^{-1}. Pion rate expected on the level less than of 5% of the electron rate. An estimate of the negative kaon rate was made by using Wiser's parametrization of experimental data [39]. It is about 90 Hz. The effective photon energy range for the process from 3.85 to 4.75 GeV. The kaon rate at the trigger detector is approximately 30 Hz due to kaon decay.

4.3 Singles rates in the BigBite

The proposed configuration of the detectors was analyzed for singles rates, which defined the maximum usable luminosity and possible production rate. This section deals with the calculation and measurement of the singles rate in the BigBite spectrometer.

Figure 6 shows the expected rate of electrons at different momenta. The proton rates are shown in Fig. 7. To cross check these calculations we made a measurement of the counting rate of a multi-wire proportional chamber located behind BigBite at 65° and a distance of 8 m from the target. During measurements the beam energy was 4.2 GeV. The observed rate was found to be about half the calculated rate [37]. In the analysis below we used the calculated rate as a conservative estimate of the background.

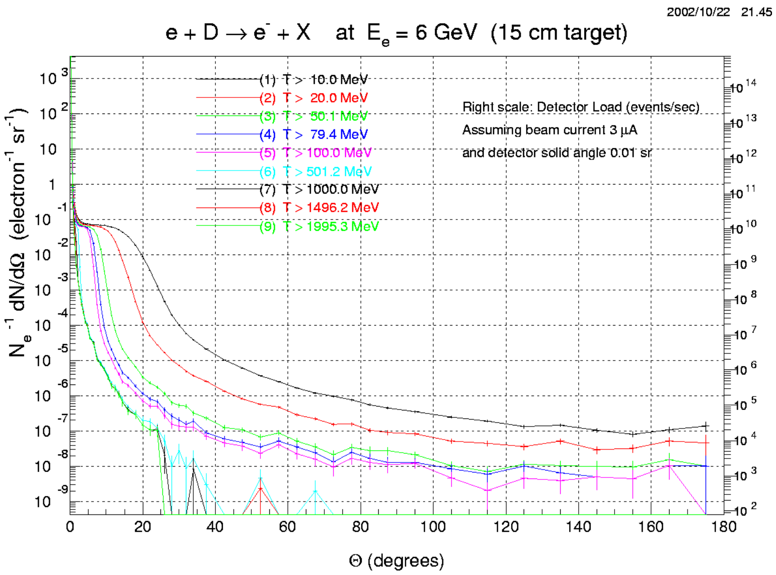

Figure 6: Electron rate at $\mathcal{L}_{eN}$ of $2.75 \cdot 10^{37}$ cm^{2}s^{-1}. The detector solid angle is 0.01 sr in this plot.

Field of 9 kG	e^-	$\pi^\pm$	kaon	proton
rate [MHz]	0.5	8.2	0.02	3.3

Table 5: The singles rates in BigBite at $\mathcal{L}_{eN}$ of $3 \cdot 10^{37}$ cm^{2}s^{-1}.

For this experiment, BigBite will be installed out of plane at average polar angle 27°, at larger than the nominal distance from the target, so the solid angle will be 26 msr. The rates integrated over the acceptance are shown in the Tab. 5. The kaon rate shown in the table includes a decay factor.

4.4 Singles rate in the neutron detector

In the proposed experiment we will use the neutron detector N-200, which is under preparation for the GEN experiment E02013 [24]. It will be installed at distance of 12 m from the target at average polar angle of 27 degree relatively beam line.

In 2002 we built a 10% segment of the full detector (20 neutron bars and 8 veto paddles) and used it for measurement of the singles rates and trigger rates at a distance of 8 m from the target and 25° from the beam line. Rates were found to be in good agreement with DINREG-based calculations [36].

Figure 8 shows the expected rate of pions at different momenta, which contribute to the rate in N-200. The rate of neutrons is shown in Fig. 9. Table 6 shows the expected detectors rates in N-200 during proposed measurement, which obtained from complete MC simulation of the setup including proposed Be target and detailed N-arm structure.

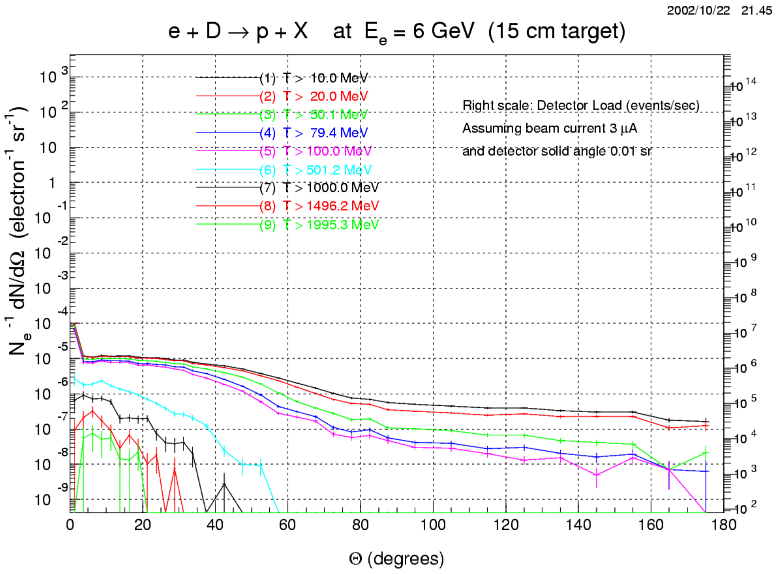

Figure 7: Proton rate at $\mathcal{L}_{eN}$ of $2.75 \cdot 10^{37}$ cm^{2}s^{-1}. The detector solid angle is 0.01 sr in this plot.

	veto paddle	N-bar PMT, above 5 MeVee	trigger, above 20 MeVee
rate [MHz]	1.2	0.06-0.18	5.7

Table 6: The rates in the neutron detector at $\mathcal{L}_{eN}$ of $3 \cdot 10^{37}$ cm^{2}s^{-1}.

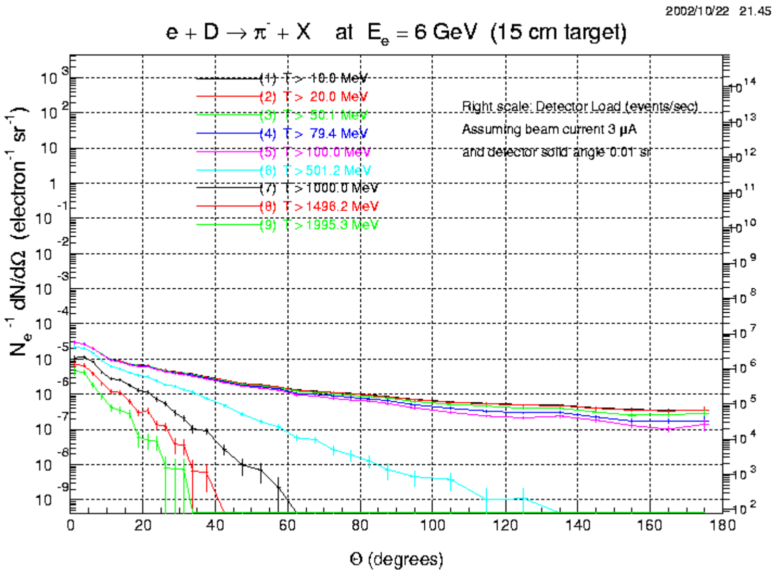

Figure 8: Pion rate at $\mathcal{L}_{eN}$ of $2.75 \cdot 10^{37}$ cm^{2}s^{-1}. The detector solid angle is 0.01 sr in this plot.

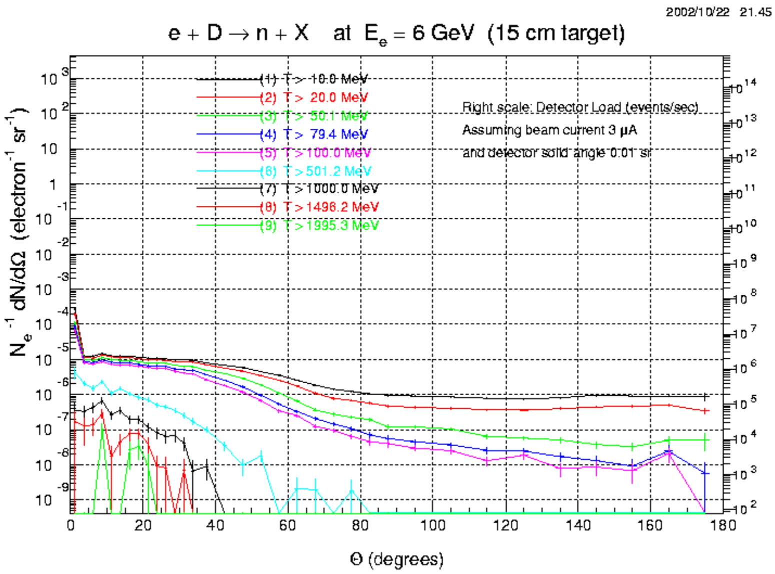

Figure 9: Neutron rate at $\mathcal{L}_{eN}$ of $2.75 \cdot 10^{37}$ cm^{2}s^{-1}. The detector solid angle is 0.01 sr in this plot.

5 Monte Carlo simulation of the experiment

There are following main parameters obtained from the MC simulation:

- the resolution for an invariant mass of the nK^+ system;
- the probability to detect decay products of Θ^+ state in N-arm and BigBite;
- the probability to detect a negative kaon in the HRS in events, when the Θ^+ particle was produced;
- the photon energy range corresponding to a negative kaon in the HRS momentum acceptance; and
- the probability to detect decay products of a system produced, when K^- is registered in HRS: a non-resonance background.

The MC code for this experiment is written under GEANT-3. The HRS spectrometer is represented by its acceptance and resolution in configuration with the septum magnet as shown in Tab. 2. Decay of the kaon on the path to the HRS detector was calculated separately. The BigBite geometry was described in many details, including geometry of the magnet and every detector. The resolution was found from additional MC study of the optics reconstruction matrix. The neutron detector was represented by its front face. N-arm detection efficiency was calculated by a separate code [38] (see Fig. 4).

5.1 The mass resolution and detection probability for the Θ^+

In the MC a photon generates an event from the nucleon, which contains a negative kaon (uniformly in the acceptance of the HRS) and a system with a mass of 1540 MeV. The system decays to a neutron and a positive kaon with isotropic distribution in its cms. Resulting event distributions are shown in Fig. 10 and Fig. 11. The mass resolution (FWHM) was found of 2.1 MeV. Figure 11 presents distributions Θ^+ events over the incident photon energy, the resonance momentum, the neutron momentum, and the correlation of the neutron and kaon momenta.

The probability for detection was found to be $f_{nK^+}^{N*BB-accept} = 1.67 \cdot 10^{-3}$ for a mass of 1.54 GeV . The detection probability for different resonance mass defines an acceptance range of the experiment. To do this the mass of produced system was generated uniformly in range from 1.4 to 1.7 GeV. The smooth background in Fig. 10 presents also a shape of acceptance in this experiment for different mass of nK^+ system.

5.2 The probability to detect negative kaon in HRS

This very important parameter was calculated by using two ways: a first is a model of the Θ^+ photo production from a neutron [45] and a second is an experimental shape of the K^+ distribution in the photo production of $\Lambda(1520)$ [46], shown in Fig. 12. The fraction of the total cross section, which corresponds to the HRS acceptance, was calculated from

$$f_{\gamma,K^-}^{HRS-accept} = \left[\frac{d\sigma}{dt}\Big|_{t-aver} \times \Delta t \times \frac{\Delta\phi}{2\pi} \right] / \sigma_{total}$$

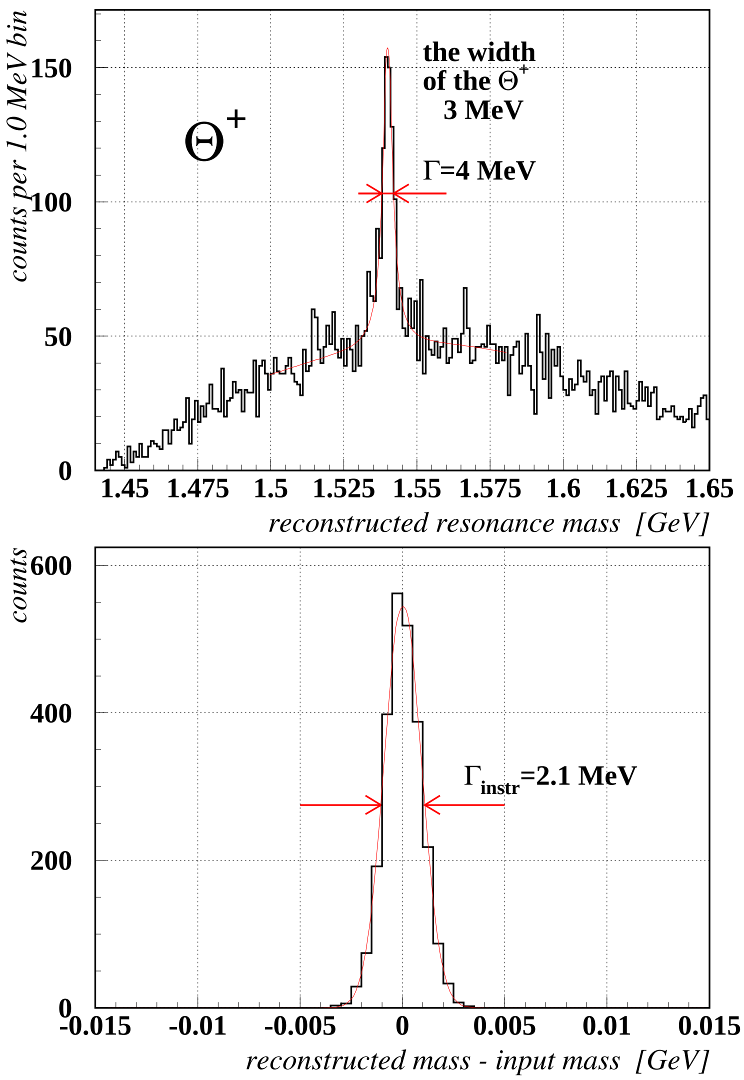

Figure 10: The acceptance and resolution for invariant mass of the nK^+ system. Statistics in this plot corresponds to the production cross section of 4.5 nb at photon energy 4 GeV.

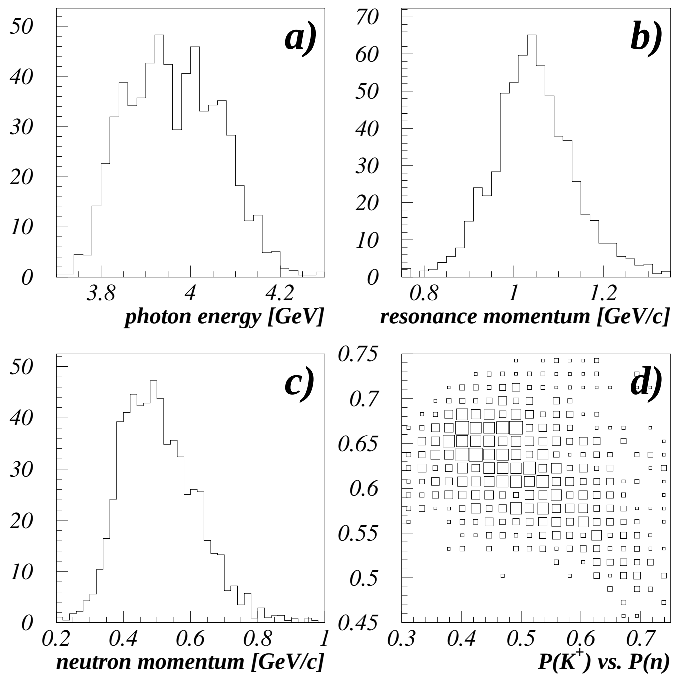

Figure 11: The event distributions for Θ^+ production a) the photon energy; b) the Θ^+ momentum; c) the final neutron momentum; and d) the correlation between the neutron and kaon momenta.

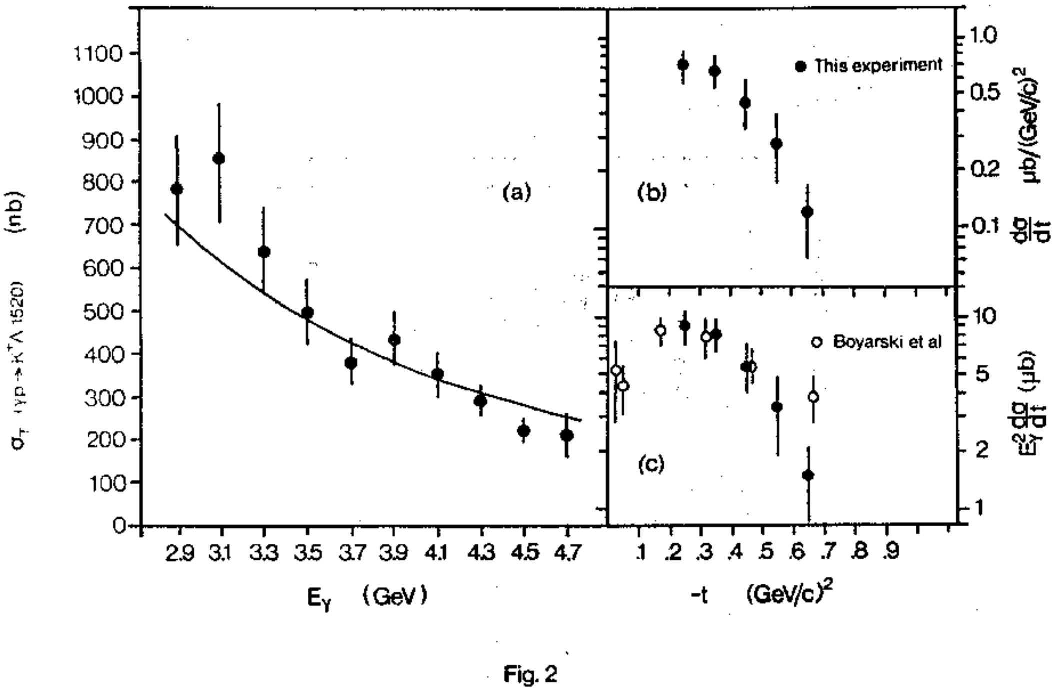

Figure 12: The total and differential cross section for photo production of $\Lambda(1520)$ from proton [46].

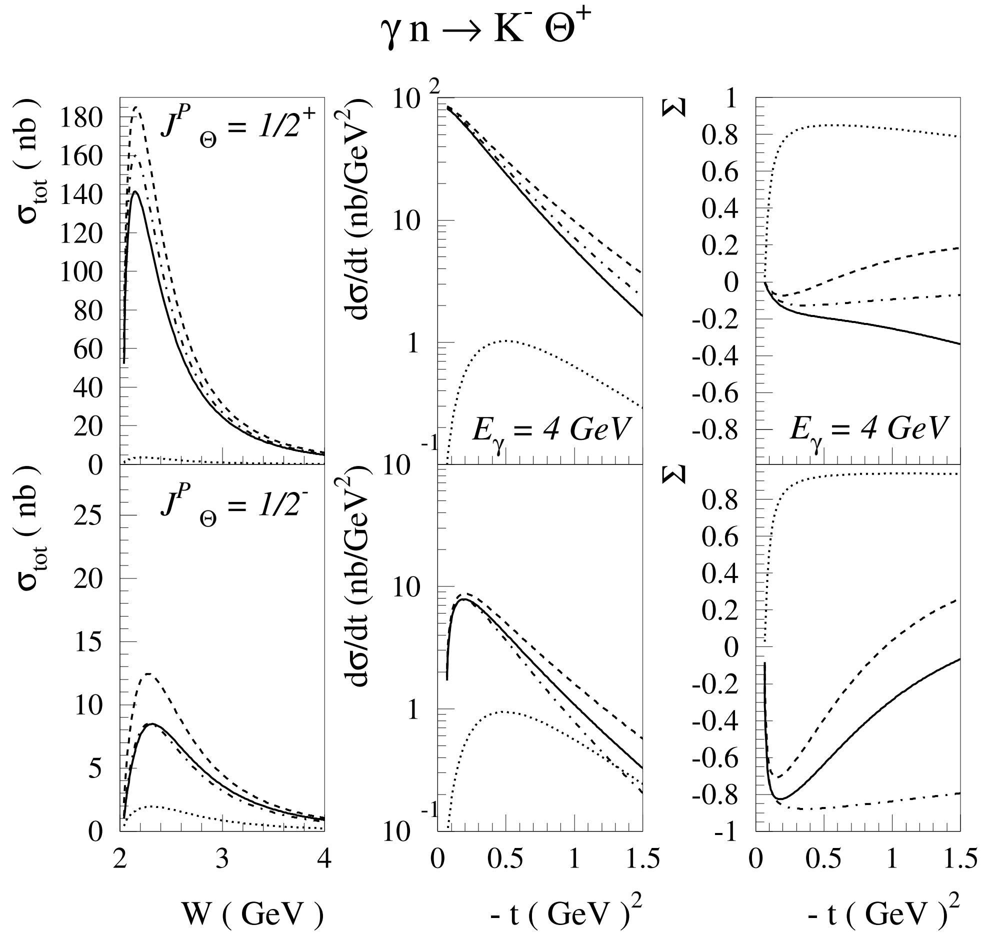

Figure 13: The total and differential cross section for photo production of Θ^+ according to [45].

where $\Delta t = 0.12$ (GeV/c)^2 is a range of t momentum transfer, which was found by the MC according to HRS acceptance, and $\Delta\phi = 0.87$ is the HRS azimuthal angle coverage. The value of $f^{HRS-accept}_{\gamma,K^-}$ was calculated by using results [45] (see Fig. 13). For positive parity the $f^{HRS-accept}_{\gamma,K^-}$ is of 0.032 and for negative parity it is 1.5 times less. The second approach with the $\Lambda(1520)$ leads to the $f^{HRS-accept}_{\gamma,K^-} = 0.031$. Thus we used the value of $f^{HRS-accept}_{\gamma,K^-} = 0.032$ for an estimation of the Θ^+ counting rate. The same result was obtained from MC of acceptance.

5.3 Non-resonance background

A starting point for the analysis is a rate of K^- in the HRS focal plane, which was found of 30 Hz (see Sec. 4). The production of K^- is associated with the production of the kaon and hadron system. At low end of the photon energy (about 3.8 GeV) such a system is a kaon and a nucleon (nK^+ or pK°). For a photon energy above 4 GeV the acceptance for three body system of a kaon, a nucleon, and a pion, opens up. The probability to have a neutron and a K^+ in the acceptance of N-arm and BigBite for the γ, K^- event has contributions from the production of both two body nK^+ and three body $nK^+\pi$ final states. The accepted fractions are $f_{nK^+}^{N*BB-accept} = 1.67 \cdot 10^{-3}$ and $f_{nK(\pi)}^{N*BB-accept} = 0.28 \cdot 10^{-3}$ (these numbers are for 100 MeV range of nK^+ mass). However, we don't know the ratio between these two channels. We can make estimates for two extreme scenarios. In the first one the two body system is responsible for all K^- events. Final number of events per 1 MeV in invariant mass spectra is of 34 for the 20 days experiment. In the second scenario the three body system produced in all K^- events. It allows for only 9 events per MeV in final spectra because of smaller acceptance and twice the number of possible channels ($nK^+\pi^\circ$, $nK^\circ\pi^+$, $pK^\circ\pi^\circ$, $pK^+\pi^-$). We assumed a 50:50 branching ratio between nK^+ and pK°, which could be effected by dynamics of the production process. We also assumed a 25% branching ratio to $nK^+\pi^\circ$ in three body final state, which again could be effected by dynamics. Resulting non-resonance background is of 34 ± 25 events per MeV.

5.4 The photon energy range and photon flux

The luminosity of Θ^+ production experiment is proportional to the photon energy range for which negative kaon could be detected by HRS and Θ^+ decay products in N-arm and BigBite. For present kinematics we found this range is from 3.8 to 4.1 GeV as shown in the upper left plot of Fig. 11.

A photon intensity was found in an approximation [41], which lead to effective radiator 0.015 radiation length. An additional radiator with thickness of 0.002 radiation length is due to Be target.

6 Proposed measurement

A measurement is proposed which will allow observation of a narrow Θ^+ state in an invariant mass spectrum with sensitivity of 1 MeV wide resonance. Experiment will measure a mass and width of the state. Experiment will also measure an angular distribution of the decay products. If the width is about 10 MeV, which leads to a large production cross section, more events will be obtained from electro production data, which covers large range of four momenta of virtual photon as well as large range of momentum transfer to negative kaon.

The key experimental elements of the present proposal are

- a high resolution spectrometer HRS in Hall A;
- a septum magnet for HRS, which allows detection of particles for the central trajectory in each spectrometer at an angle of 6°;
- a large acceptance magnetic spectrometer BigBite, with a high resolution detector package under construction for the GEN experiment;
- a large array of the neutron counters, which is also a part of the GEN experimental setup;
- a 50 cm long multi foil Be target; and
- a set of threshold Čerenkov counters for PID in BigBite.

The primary goal of proposed experiment will be realized by using photo production by quasi-real photons. The flux of quasi real photons may be calculated [41], which will allow for the determination of the production cross section, which is still undertermind in spite of dozen published observations of the Θ^+ state. The high energy forward negative kaon presents a very important **tag**, which reduces dramatically the contribution of competing reactions into K^+-neutron event sample and selects sample of slow Θ^+ , which allow for the accurate measurement of its mass. Exact photo-production mechanism of the Θ^+ is unknown. However, it is logical to expect that it is similar to the t-channel dominated process for producing the $\Lambda(1520)$. The important parameters in this case are the total cross section and its t-dependent slope. In the calculation of the acceptance we used a predictions [45] and an experimental shape of the differential cross section from the process $\gamma p \to K^+\Lambda(1520)$.

The electro production measurement, which does not require extra beam time and, as a result, is not discussed in details in this text, could be quite useful in case Θ^+ has large width and production cross section. The post-target tagging approach, often used in hypernuclei experiments, is a low Q^2 electro-production study of photo-production processes. The effective flux of photons is also much higher than achievable with a tagged real photon beam if the electron scattering angle is sufficiently small. The cross section may also have large a σ_{TT} term, where the ratio to the σ_T is related to the Σ photon polarization observable and can be estimated from parasitic electro production experiment because of significant out-of-plane acceptance. For small scattering angles the effective degree of linear photon polarization can be presented as $(1 + E_\gamma^2/(2E_e^i E_e^f))^{-1}$ which is ≈80% for the conditions of this measurement.

We are going to study the reaction Be$(e, nK^+K^-)X$. The concept of the measurement is shown in Fig. 2. An electron beam with a current of 30 μA at an energy of 5.0 GeV will be used. The negative kaon (or scattered electron) will be detected in the magnetic spectrometer HRS-left at a central angle of 6° with a septum magnet. The positive kaon will be detected in the BigBite spectrometer at horizontal/vertical angles 18.4°/-20°, and the neutron will be detected in the large neutron detector at horizontal/vertical angles 18.4°/+20°. The invariant mass resolution (FWHM) for nK^+ is about 2.1 MeV.

6.1 The calculation of the Θ^+ production rate

We assumed the resonance width (FWHM) of 3 MeV. In calculating the Θ^+ production rate we used the value of the total photo-production cross section of 4.5 nb motivated by analysis [45], where at 4 GeV photon energy such cross section corresponds to the width of the resonance Γ of 3 MeV. The calculations for the production and background are made for the electron-nucleon luminosity $\mathcal{L}_{eN}$ of $3 \cdot 10^{37}$ cm^{-2}s^{-1}. The photon-neutron luminosity was calculated as (see definitions in Sec. 4)

$$\mathcal{L}_{\gamma n(eutron)} = \frac{N}{A} \cdot 0.017 \cdot \frac{\Delta E_\gamma}{E_\gamma} \cdot \mathcal{L}_{eN} \approx 6.9 \cdot 10^{-4} \cdot \mathcal{L}_{eN} \;=\; 2.1 \cdot 10^{34} \text{ cm}^{-2}\text{s}^{-1},$$

where E_γ and ΔE_γ are defined by the kaon momentum and its range accepted in HRS-left, $\langle E_\gamma \rangle = 4.0$ GeV and $\Delta E_\gamma = 0.29$ GeV; $\mathcal{L}_{eN}$ is the electron-nucleon luminosity, $\mathcal{L}_{eN} = 3 \cdot 10^{37}$ cm^{-2}s^{-1}. Such a value of $\mathcal{L}_{\gamma n(eutron)}$ is about 10^4 times higher than what one can obtain with real-photon tagging. This leads to the production rate

$$\nu^{\Theta^+}_{\gamma,K^- nK^+} = \mathcal{L}_{\gamma n} \cdot \sigma^{\Theta^+}_{\gamma n} \cdot f^{HRS-accept}_{\gamma,K^-} \cdot f^{decay}_{K^-} \cdot f^{N*BB-accept}_{nK^+} \cdot \eta_n \cdot b_{nK^+} \;=\; 17 \text{ events per day},$$

where $\sigma^{\Theta^+}_{\gamma n}$ is the cross section of 4.5 nb; the $f^{HRS-accept}_{\gamma,K^-}$ is a fraction of K^- associated with Θ^+ production within HRS angular acceptance, it is ≈0.032; $f^{decay}_{K^-} = 0.31$ is the survival probability of a K^- after a 27 meter path in the HRS; $f^{BB*N-accept}_{nK^+}$ is a fraction of Θ^+ events when both decay products are in angular acceptance of N-arm and BigBite detectors, $f^{BB*N-accept}_{nK^+}$ is $\approx 1.67 \cdot 10^{-3}$; $\eta_n = 0.25$ is the detection efficiency of the neutron; and b_{nK^+} is the branching ratio for Θ^+ decay to nK^+, $b_{nK^+} = 0.5$.

By using this rate and expected non-resonance (see below) one can find a sensitivity of 20 day experiment to resonance with cross section of 1.5 nb. Random origin of similar bump will require 5-7 sigma statistical fluctuation. Another words the experiment will collect of 15 events per nb of the cross section, when we referring to the cross section at its maximum near 2 GeV photon energy.

6.2 Trigger rate and event analysis

The DAQ trigger will use a coincidence between HRS and BigBite. At forward angle and 3 GeV/c central momentum of HRS a pion rate is less than few percent of the electron rate, which is about 120 kHz at proposed luminosity. A rejection factor of the electrons and pions in HRS-left is on the order of 10^4 based on use of the gas Čerenkov and shower counters. After RICH information analysis the event sample will have less than 10% pions, the rest being kaons. The raw scintillator rate at BigBite expected to be about 12.5 MHz mainly pions and protons. On-line veto from a thin scintillators allows for the rejection of protons with kinetic energy below 100 MeV. A BigBite trigger (segmented into 24 scintillators and

24 aerogel cells) will have rate of 100 kHz, when we assumed an on-line rejection factor of 100 with two layer Čerenkov counters (see Sec. 3). Within 120 ns coincidence time window these rates lead to comfortable for DAQ accidental coincidence rate of 15 Hz.

Off-line analysis of PID detectors should bring the rejection factor for protons and pions to the level of 10^4. Most of remaining accidental events will be between a negative kaon in HRS and a positive kaon in BigBite, which has a rate of 0.05 Hz. Analysis of the event vertex (HRS-left vs BigBite) allows us to cut this accidental rate by an additional factor of 10-20 to the level of 0.005 Hz.

With 6 MHz rate of neutrons and 25% detection efficiency we expecting about 1.5 MHz rate of triggers in the N-arm after applying veto cut. It leads to 11% probability of accidental hit in 75 ns time interval, where we are expecting a neutron with momentum from 0.3 to 0.7 GeV/c. The distribution of accidental events in nK^+ invariant mass has a width of 300 MeV resulting to accidental background of very low level level of $2 \cdot 10^{-6}$ Hz/MeV or 3 event/MeV in final invariant mass spectra (after 20 days experiment).

A tracking system of BigBite has three planes of wire chambers, which are designed to handle the track rate on level of 10 MHz. For 150 ns maximum drift time we are expecting to have 1.5 extra tracks per events. Three wire chambers located in field free area allow to identify hits related to individual tracks. Tracks unrelated to the trigger will have large mismatch in drift time for left and right cells, so can be removed with a factor of 10-15. In addition a correlation of the track position and the hit position in the segmented trigger plane allow to reduce false track background by a factor of 20.

6.3 The correlated rates

The correlated rate due to real coincidences between the HRS-left, BigBite, and the neutron detector in principle has contribution from the following two reactions

- production of heavy hyperons Λ and Σ which have about 20% probability of decay in nK^+; and
- production from neutron of the ϕ meson, which decay to K^+K^- and direct production of K^+K^- pair.

However, large momentum of the negative kaon yields non-zero probability only for direct production of nK^+K^-. The MC simulation logic for the background was discussed in Sec. 5.

7 Calibration of the mass scale and resolution

Several calibration methods will be used. The list of reactions applicable in our experiment includes:

- Elastic electron scattering.
- Electro disintegration of the Deuterium - $D(e, e'n)p$ with reconstruction missing proton mass. Reconstruction of the missing neutron mass in $H(e, e'\pi^+)n$ reaction and $H(e, e'n)\pi^+$ with reconstruction missing pion mass.
- Reconstruction of the missing mass of $\Lambda(1116)$, $\Lambda(1520)$ and $\Sigma^\circ(1193,\ 1385)$ in reaction $H(e, e'K^+)X$. Reconstruction of the invariant mass of $\Sigma^+(1189)$ in reaction $H(e, e'n\pi^+)\overline{K}$. Reconstruction of the missing neutron mass in reaction $D(e, e'n\pi^+)n$ and Σ^- invariant mass in $D(e, e'n\pi^-)K^+p$. Reconstruction of the $\Lambda(1116)$ in $n\pi^\circ$ invariant mass in reaction $H(e, e'nK^+)\pi^\circ$ and a missing mass in reaction $H(e, e'K^+)\Lambda(1116)$.

During these measurements the positions of spectrometers will be the same as in the main part of the experiment. Multi-foils Be target will be used for calibration of the optics for both spectrometers. Hydrogen and Deuterium target will be used to do calibration with K^+/π^+ in several reactions.

The first method of calibration is based on elastic electron scattering from carbon and hydrogen and allows calibration of the momentum and angles reconstruction of HRS-left and BigBite. The beam with energy of one pass will be used for BigBite calibration. The expected rate is about 5 kHz at luminosity of $\mathcal{L}_{eN} = 1 \cdot 10^{35}$ cm^{-2}s^{-1}. The beam with energy of 3 GeV pass will be used for HRS calibration. Here expected rate is about several kHz at the same luminosity. Absolute beam energy will be measured by using EP system with precision of 2×10^{-4} [47].

For the neutron arm similar initial calibration of the Time-of-Flight (ToF) will be achieved by using a prompt gamma production. This calibration will be done in single arm DAQ mode as well as for main body of collected data, where N-arm trigger will be not used for on-line event selection.

The second method will check calibration of the neutron arm via reconstruction of the missing proton mass. We plan to take data for 4 hours during 0.8 GeV running conditions with HRS-left momentum adjusted to 0.5 GeV/c. The rate of 100 Hz will allow detailed test and calibration of the N-arm.

The third group of calibrations will use electro production of the hyperons. We plan to take data for 4 hours for K^+ electron production with beam energy of 3 GeV and HRS-left momentum adjusted to 1.7 GeV/$c$for detecting scattered electron. Additional calibrations will be done with beam of 5 GeV for total of 40 hours of beam time. During 5 GeV calibration run we will use several HRS settings. A setting of 3.7 GeV/c provides data on the Σ^+ invariant mass.

We present below the MC result for the process - $H(e, e'K^+)\Lambda(1116)$ The distributions shown in Fig.14 are generated from MC simulated data. The missing mass resolution (FWHM) of 4.2 MeV will test the BigBite performance for detecting K^+.

The Σ^+ production will provide a very detailed test through the reconstruction of invariant its mass. The difference in masses between the Θ^+ and Σ^- resonances is 350 MeV, which is close to mass difference between a kaon and a pion. The data taking will be done for HRS

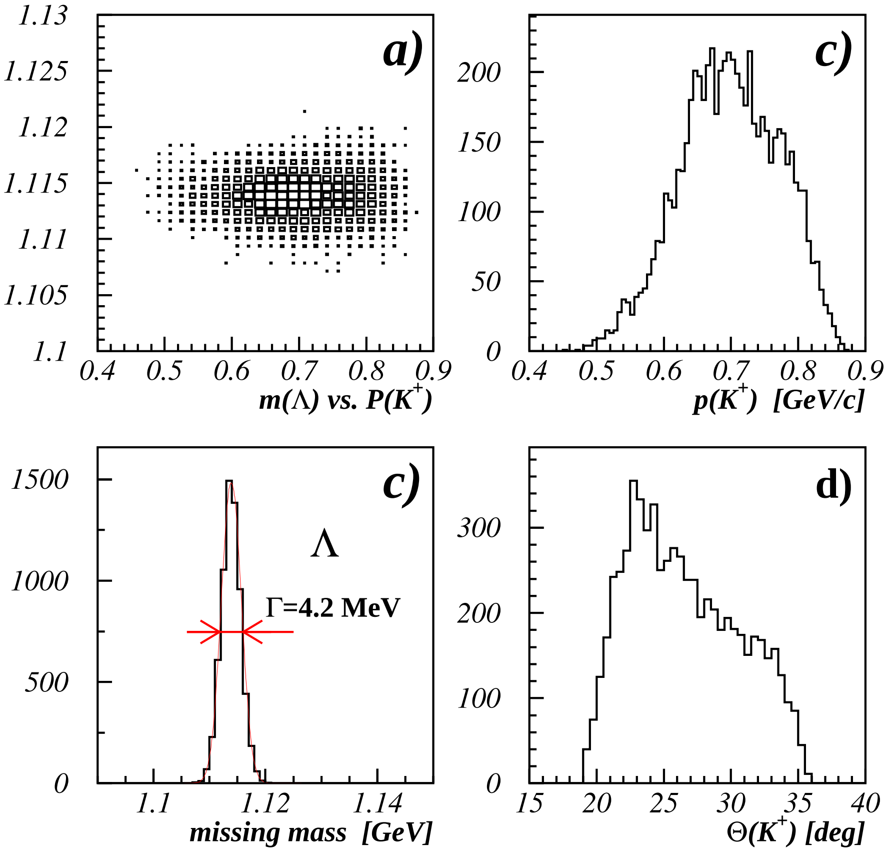

Figure 14: The event distributions from K^+ production run with missing $\Lambda(1116)$.

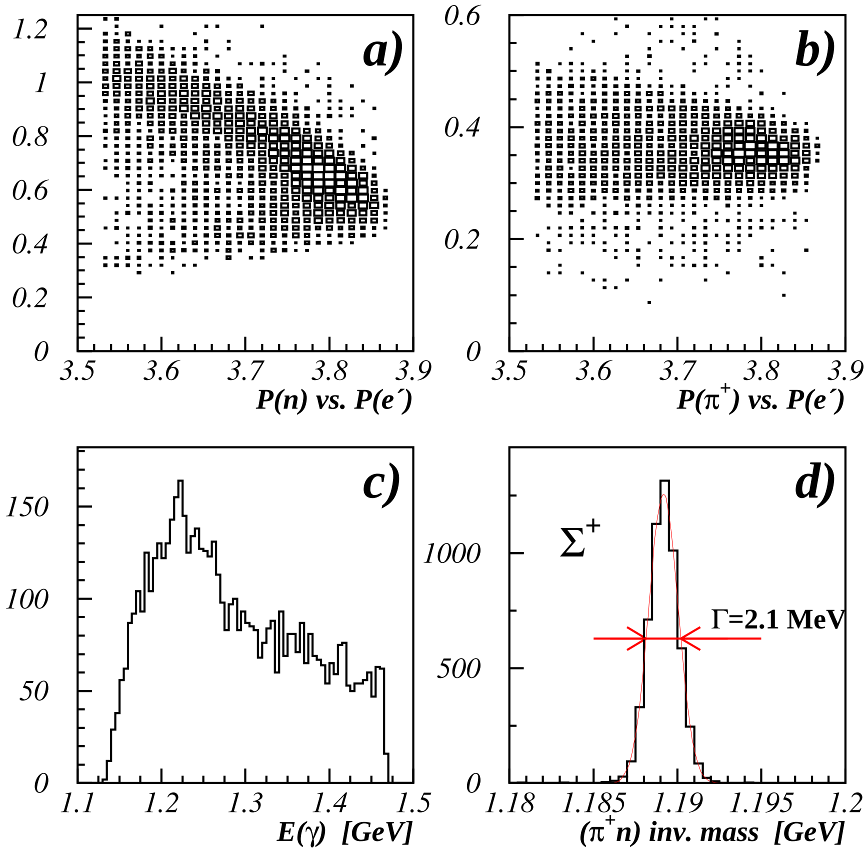

Figure 15: The event distributions for Σ^+ production a) the neutron momentum vs the final electron momentum; b) the π momentum vs the final electron energy; c) a photon energy spectra; and d) a Σ peak in the invariant mass spectra of $n\pi^+$.

momentum of 3.7 GeV/c. The momentum and mass distributions are shown in Fig.15. Such level statistics will be collected in 12 hours of beam time. The invariant mass resolution (FWHM) for Σ^- is 2.1 MeV.

8 Productivity at different values of t

8.1 Cross section's t dependence

Production mechanism of the Θ^+ is unknown, and even its existence still need to be proven. There is a large body of theoretical papers where possible production mechanisms are discussed. Most of them using a theory of hyperon photo production as a guidance for construction of the Lagrangian and selection of the coupling constants. Low-t dominance in photo production predicted in Regge type calculations [45] shown in the Fig. 13. Some calculations (for example [44]) predicted enhancement at large t. Most experimental observations come from forward angle experiments [3, 5, 9], which is suggestive that forward angle, low t setup is preferable place to look for the pentaquark signal.

8.2 Acceptance vs t range

The proposed experimental setup could be used at different values of t. We focus this proposal on quite small momentum transfer of -0.22 (GeV/c)^2 with average $\theta_{cm}^{K^-} = 21°$, but if at the time of data taking will be indications that larger angle provides higher counting rate we can just change angles of the detectors and reach higher t value. Figure 16 shows the

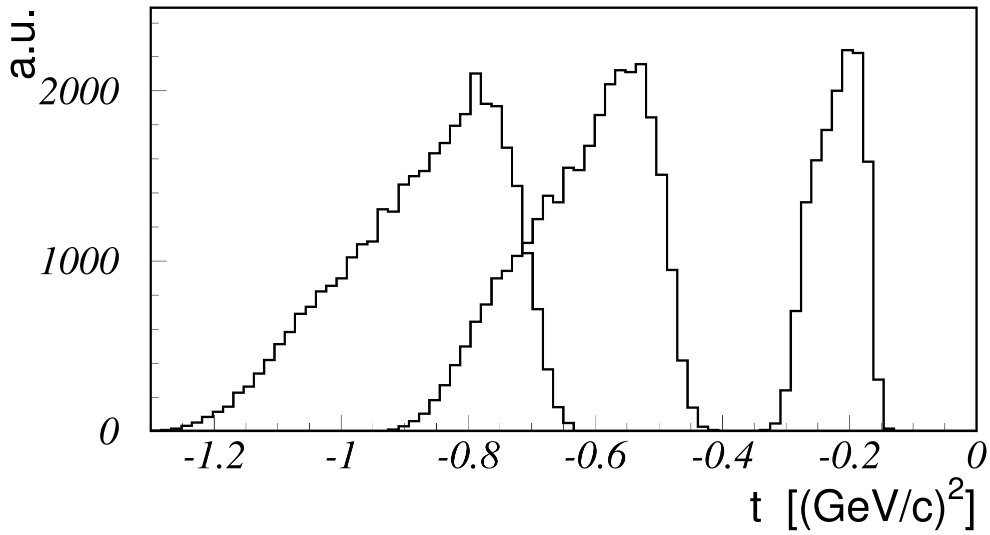

Figure 16: The event distributions over t in proposed experiment for three possible settings of K^- spectrometer.

acceptance coverage in $\theta_{cm}^{K^-}$ for three different positioning of the spectrometer. Table 7 shows the production rate and the factors, which used to calculate counting rate of Θ^+ events.

Tab. 7 shows that at larger $-t$ the acceptance of HRS is lowering, see a parameter $\Delta\sigma/\sigma_{tot} = f_{\gamma,K^-}^{HRS-accept}$, in the case of low t dominance, but growing in the model [44]. The same time the acceptance of the BigBite-N-arm is increasing, see a parameter $f_{nK^+}^{BB*N-accept}$,

Configuration #		1	2	3
$\theta_{cm}^{K^-}$	[degree]	21	40	48
$-t_{aver} - t_{min}$	[(GeV/c)^2]	0.15	0.55	0.81
$\theta_{lab}^{K^-}$	[degree]	6	12.5	15.0
θ_{N-arm}	[degree]	$18.4/+20$	$25/+20$	$27/+20$
$\theta_{BigBite}$	[degree]	$18.4/-20$	$25/-20$	$27/-20$
$\langle E_\gamma \rangle$	[GeV]	3.95	3.95	4.1
ΔE_γ	[GeV]	0.29	0.35	0.37
$\Delta\phi_{_{HRS}}$	[radian]	0.87	0.60	0.50
Δt	[(GeV/c)^2]	0.12	0.27	0.35
$f_{K^-}^{decay}$		0.31	0.28	0.28
$\Delta\sigma/\sigma_{tot} = f_{\gamma,K^-}^{HRS-accept}$	[45] (Regge model)	0.032	0.015	0.007
$\Delta\sigma/\sigma_{tot} = f_{\gamma,K^-}^{HRS-accept}$	[46] ($\Lambda(1520)$)	0.031		
$\Delta\sigma/\sigma_{tot} = f_{\gamma,K^-}^{HRS-accept}$	[42] (data for $\Lambda(1520)$)	0.031	0.032	
$\Delta\sigma/\sigma_{tot} = f_{\gamma,K^-}^{HRS-accept}$	used in proposal	0.032	0.015	0.007
$f_{nK^+}^{BB*N-accept}$		0.0017	0.0031	0.0044
mass resolution, FWHM	[MeV]	2.1	2.6	3.0
$\Delta\sigma(\gamma n, K^-\Theta^+)$	[fb] (used)	9.4	8.1	5.4

Table 7: Parameters of the experiment for three possible configurations of the detectors and production cross sections.

because a larger value of $-t$ leads to focusing of the Θ^+ decay products into the detector acceptance. As result the production cross section, see a parameter $\Delta\sigma(en, K^-\Theta^+)$, drops just by a factor of 1.7 or less (in the model [44]). Because for large angles of the detectors the useful luminosity could be higher a loss of the cross section is partly compensated. The mass resolution for higher $-t$ become worth however it is still have FWHM = 3.0 MeV.

item	type of measurement	current [μA]	energy [GeV]	time [hr]
1	BigBite and N-arm calibration	30	0.8	12
2	beam energy measurement	1	3.0	4
3	HRS and BigBite(K) calibration	30	3.0	8
4	beam energy measurement	1	5.0	6
5	mass resolution calibration	30	5.0	40
6	Θ^+ production run	30	5.0	480
total				550

Table 8: The time allocation assuming 100% efficiency.

9 Expected results and beam time request

9.1 Search for narrow resonances

This experiment has unique sensitivity in the search of narrow resonances decaying to nK^+ in mass range 1500-1600 MeV. The resonance with the width of 1 MeV (total photo production cross section of 7 nb at 2 GeV photon energy) will be observed as a signal 5-7 times larger statistical fluctuation. The expected search example is shown in Fig. 17.

9.2 The mass and width of the Θ^+ state

The systematic accuracy of mass measurement of 0.5 MeV was estimated from systematics of calibration which will be done by using several methods with large statistics for Λ and Σ resonances. With 340 events, which are expected for the 3 MeV width of the resonance, will allow for 0.2 MeV uncertainty.

For the width $\Gamma_{res} = 3$ **MeV the experimental result will be** 3.0 ± 0.7 **MeV**. The expected mass distribution is shown in Fig. 18.

9.3 Beam time request

The purpose of this experiment is to search for and measure the parameters of the the Θ^+ state. The experiment will be performed at beam energy 5.0 GeV, with currents up to 30 μA. Table 8 summarizes the beam time requirements. The measurement needs installation of the detectors constructed for experiment E02013 [24] in out-off-plane configuration. In total we request 23 days of beam-time to perform the proposed measurements.

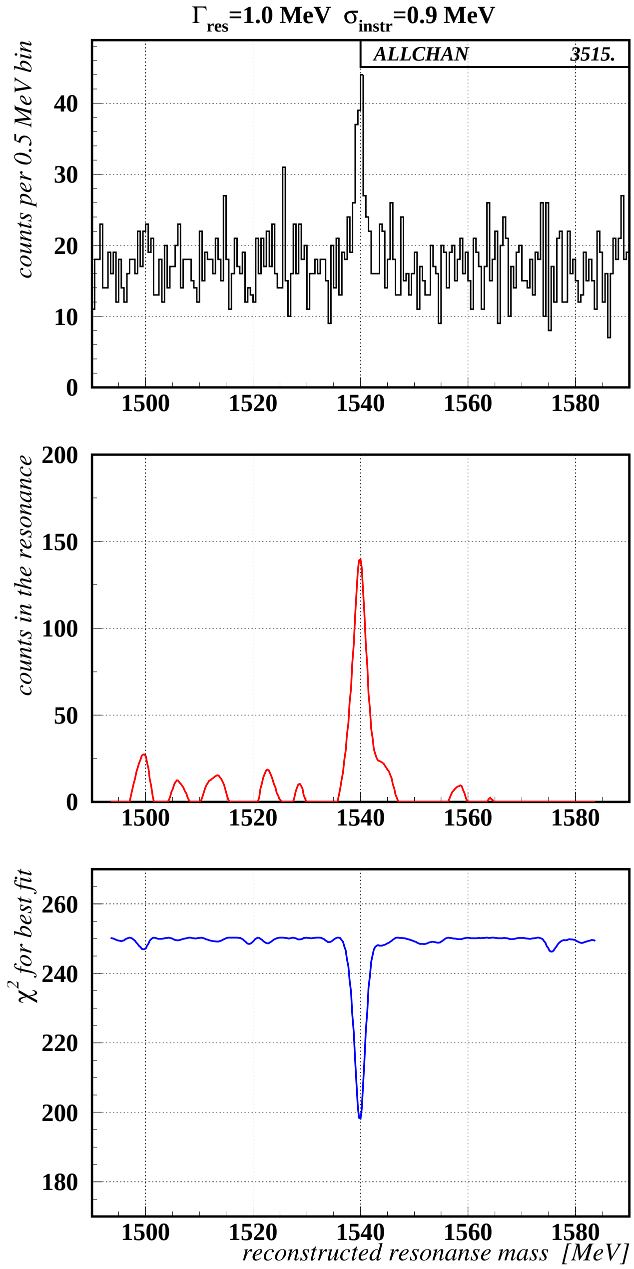

Figure 17: The MC data and a search for 1 MeV wide resonance. A top panel shows the data. A middle panel shows the amplitude of the peak which allow best χ^2. A bottom panel shows the value of χ^2 when position of resonance scan through the region.

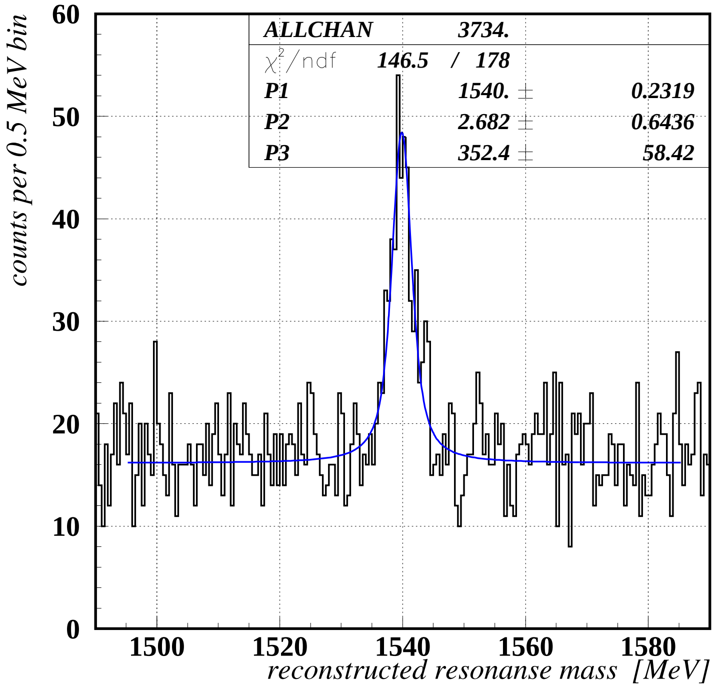

Figure 18: The MC data and a fit for 3 MeV wide resonance.

10 Conclusion

We request 550 hours of beam-time to search for the resonances and measure their mass and width in reaction Be$(e, nK^+K^-)X$ at photon energy of 4 GeV. Collected data will allow also us to conduct a study of the Θ^+ electroproduction in reaction $(e, e'nK^+)$. Measurement of the width with an instrumental resolution (FWHM) of 2.1 MeV will reveal the state's width and enhance our understanding of the nature of Θ^+ exotic state. The value of the mass will be established with an accuracy of 0.5 MeV. Furthermore, the proposed experiment will collect a sample of about 340 Θ^+ events (for an assumed 3 MeV resonance width) and investigate the resonance properties. We propose an experiment which can firmly establish the resonance even if its width of 1 MeV (which corresponds to the total photo production cross section of 7 nb at its maximum near 2 GeV photon energy). The status of the equipment needed in the proposed measurements should permit the experiment to be realized in a time scale of one year. Additional resources may allow a reduction in preparation time. All known experiments have at least several times lower mass resolution and sensitivity than this proposal.

References

[1] Charles Seife, Science **306**, 19 November, p1281 (2004).

[2] D. Diakonov, V. Petrov, and M. Polyakov, *Z. Phys. A.* **359**, 305 (1997).

[3] T. Nakano *et al.*, *Phys. Rev. Lett.* **91**, 012002 (2003).

[4] V.V. Barmin *et al.*, Phys. Atom. Nuclei **66**, 1715 (2003).

[5] S. Stepanyan *et al.*, *Phys. Rev. Lett.* **91**, 252001 (2003).

[6] V. Koubarovsky *et al.*, *Phys. Rev. Lett.* **92**, 032001 (2004).

[7] J. Barth *et al.*, *Phys. Lett.* **B572**, 127 (2003).

[8] A. E. Asratyan *et al.*, Phys. Atom. Nuclei **67**, 032001 (2004).

[9] A. Airapetian *et al.*, *Phys. Lett.* **B585**, 213 (2004).

[10] M. Abdel-Bary *et al.*, [COSY Collaboration], hep-ex/0403011.

[11] A.Aleev et al., [SVD Collaboration], hep-ex/0309042.

[12] R. Jaffe and F. Wilczek, hep-ph/0307341.

[13] M. Karliner and H. J. Lipkin, hep-ph/0307243.

[14] E. Shuryak and I. Zahed, hep-ph/0310270.

[15] F. Stancu and D. O. Riska, *Phys. Lett.* **B575**, 242 (2003).

[16] S. Nussinov, hep-ph/0307357.

[17] R. A. Arndt, I. I. Strakovsky, and R. L. Workman, *Phys. Rev. C* **68** , 042201 (2003).

[18] Robert N. Cahn and George H. Trilling, Phys. Rev. D **69**, 011501(R) (2004).

[19] Robert Jaffe, private communication.

[20] W. Liu and C. M. Ko, Phys. Rev. C **68**, 045203 (2003).

[21] W. Liu and C. M. Ko, arXiv:nucl-th/0309023 (2003).

[22] J. Haidenbauer and G. Krein, hep-ph/0309243, to be published in *Phys. Rev. C* .

[23] C. Alt *et al.*, [NA49], submitted to *Phys. Rev. Lett.* , hep-ex/0310014.

[24] G. Cates, B. Reitz, K. McCormick, and B. Wojtsekhowski, spokespersons, JLab experiment E02-013.

[25] K. Hicks, report on APS meeting, April, 2004.

[26] K. Hicks and S. Stepanyan, spokespersons, JLab experiment E03-113.

[27] M. Battaglieri, R. De. Vita, and V. Kubarovsky, spokespersons, JLab experiment E04-021.

[28] B. Wojtsekhowski and P. Reimer, spokespersons, JLab proposal P04-012 for PAC25.

[29] PAC25 report, http://www.jlab.org/exp prog/PACpage/pac.html .

[30] G. Cates, P. Souder, and B. Wojtsekhowski, JLab LOI 04-004 for PAC25.

[31] F. Garribaldi, private communication (2003).

[32] D. J. J. de Lange *et al.*, *Nucl. Instr. Meth.* A **406**, 182 (1998); D. J. J. de Lange *et al.*, *Nucl. Instr. Meth.* A **412**, 254 (1998).

[33] L. Tang *et al.*, HKS report for JLab readiness review, (2003).

[34] P. V. Degtyarenko, "Applications of the Photo-nuclear Fragmentation Model to Radiation Protection Problems", Proceedings of the Second Specialist's Meeting on Shielding Aspects of Accelerators, Targets and Irradiation Facilities (SATIF2), 12-13 October 1995, CERN, Geneva, Switzerland, p. 67; P. V. Degtyarenko, M. V. Kossov, and H-P. Wellisch, Chiral Invariant Phase Space Event Generator, I. Nucleon-antinucleon annihilation at rest, Eur. Phys. J. A **8**, p. 217 (2000).

[35] B. Wojtsekhowski, P. Degtyarenko, R. Lindgren, "A New Tool For Correlation Studies in Hall A at JLAB, JLab-TN-01-047", report on 5th Workshop on Electromagnetically Induced Two-Hadron Emission, Lund, Sweden, (2001).

[36] P. V. Degtyarenko, GEN collaboration meeting, May 24, 2003, http://hallaweb.jlab.org/experiment/E02-013/collabmeetings.html.

[37] P. V. Degtyarenko, GEN collaboration meeting, 10/24/2003,

[38] I. A. Rachek, GEN collaboration meeting, 10/24/2003.

[39] D. Wiser, Ph.D. thesis, University of Wisconsin, 1977.

[40] H. Burfeint *et al.*, *Phys. Lett.* **43B**, 345 (1973).

[41] H. Burfeint *et al.*, *Nucl. Phys.* **B74**, 189 (1974).

[42] A. M. Boyarski *et al.*, *Phys. Rev. D* **14**, 1733 (1976).

[43] V. M. Budnev *et al.*, *Phys. Rep.* **15**, 181 (1974).

[44] Y. Oh, H. Kim, and S. H. Lee, hep-ph/0312229.

[45] M. Guidal, M. V. Polyakov, and M. Vanderhaeghen, report on the Pentaquark workshop, JLab 11/6-8, 2003 and private communication.

[46] D. P. Barber *et al.*, Z.Phys **C7**, 17 (1980).

[47] J. Alcorn *et al.*, *Nucl. Instr. Meth.* A **522** 294-348 (2004).